

# Wakefield Driven by the Strongly Accelerated Beam of an RF Photoinjector

J.-M. Dolique

*LPPG. Université Joseph Fourier-Grenoble I  
BP 53, 38041 Grenoble Cedex 9  
and CEA-PTN  
BP 12-91680 Bruyères-le Châtel  
France*

## Abstract

The wakefield map  $\mathbf{E}, \mathbf{B}(\mathbf{x}, t)$  generated by a charged particle beam, moving at constant relativistic velocity, along a pipe has been numerically calculated for many cavity geometries, and analytically expressed for a cylindrical "pill box" cavity. In RF photoinjectors used as high quality, high intensity short beam sources, one is faced with a new wakefield problem : the wakefield of strongly accelerated particles which, extracted from the cathode with thermal velocities, become relativistic before they leave the cavity. For a cylindrical cavity, the wakefield map corresponding to this situation is analytically deduced from Maxwell's equations by both integral transform and Green's function techniques. Results are found in excellent agreement with those obtained elsewhere by a time-dependent normal mode analysis [1]. Numerical applications are given for the photoinjector of the CEA facility "ELSA"[2].

## 1 INTRODUCTION

Wakefields generated by charged particle beams travelling inside conducting cavities have been the subject of several numerical approaches, and of a some analytical theoretical works, when the cavity geometry has been simple enough to allow it. These works are all related to coasting beams and cannot be applied to a strongly accelerated beam, like a photoinjector beam, the velocity of which increases from thermal to relativistic values in a few centimeters. This is particularly true for the time-dependent normal mode analysis, the only method which, for a cylindrical "pill-box" cavity, has led not only to wake potentials (which describe a global effect after the beam has crossed the cavity) but to explicit expressions of the wakefield map  $\mathbf{E}, \mathbf{B}(\mathbf{x}, t)$  (e.g. [3]).

A modified time-dependent normal mode analysis, taking into account beam acceleration, is presented in a companion paper [1].

The aim of the present communication is also the theoretical description of the wakefield for an intense electron beam, strongly accelerated inside a cylindrical cavity like the one of a photoinjector. The approach however will be different. By using both integral transform and Green's function methods, Maxwell's equations are solved in the space-time domain, taking into account boundary conditions on the cavity walls, without recourse to developments in normal modes.

Field expressions will be computed for the photoinjector of the CEA-PTN "ELSA" facility [2], and compared to those obtained from the normal mode analysis [1].

## 2 STARTING EQUATIONS. MODELLING

We solve Maxwell equations for potentials, in Coulomb gauge:  $\Delta\Phi = -\rho/\epsilon_0$ ,  $\square\mathbf{A} = \mu_0\mathbf{j} - (1/c^2)(\partial/\partial t)\nabla\Phi$  in the axisymmetric cylindrical cavity  $\mathcal{D}$  ("pill box") :  $0 \leq z \leq g$ ;  $0 \leq r \leq \mathcal{R}$ .

The initial conditions at emission beginning,  $t=0$ , are :  $\Phi=0$ ,  $\mathbf{A}=0$ ;  $\partial\Phi/\partial t=0$ ,  $\partial\mathbf{A}/\partial t=0$ . On the border  $\partial\mathcal{D}$ , which is the conducting cavity, the boundary conditions are : Dirichlet conditions for  $\Phi$  and the tangential component of  $\mathbf{A}$  :  $\Phi=0$ ,  $\mathbf{A}_t=0$ , and Neumann conditions for the normal component of  $\mathbf{A}$  :  $\partial\mathbf{A}_n/\partial n=0$

The source terms :

$$\rho(r, z, t) = \frac{I\varpi(z, t)}{\pi a^2 \beta(z) c} [1 - H(r - a)],$$

$$\mathbf{j}(r, z, t) = \beta(z) c \rho(r, z, t) \mathbf{u}_z$$

describe a radially uniform beam of radius  $a$  and velocity  $v(z) = \beta(z)c$ , carrying a total current  $I$  with an arbitrary longitudinal current profile  $\varpi(z, t)$  ( $H$  : Heaviside)

The RF accelerating electric field is assumed to be constant, which is a good approximation for the photoinjector of "ELSA", the working frequency of which is 144 MHz, as long as the pulse duration  $\tau$  satisfies  $\tau \ll 7$  ns.

## 3 BRIEF OUTLINE OF THE CALCULATIONS. ANALYTICAL RESULTS

Both equations in the Coulomb-gauge potentials quoted above are solved by integral transform and Green's function techniques. Fields are then deduced, their only non-vanishing components being, according to symmetries :  $E_z$ ,  $E_r$ , and  $B_\theta$ .

Though an arbitrary axial current profile could be treated, we restrict the following results, for sake of simplicity, to a beam pulse of time length  $\tau$ , with stiff front- and back-current profiles.

Reduced coordinates and quantities will be used, based upon the characteristic length  $H^{-1} = mc^2/eE_0$ , where  $e$  and

$m$  are the electron charge and mass respectively, and  $E_0$  the RF-electric field amplitude on the photoinjector cathode:  $R=Hr, Z=Hz, \rho=H\rho, G=Hg; T=Hct, T=Hc\tau, A=Ha$ .

Field expressions depend on whether the beam is entirely extracted or not, and whether the considered point is located inside the beam or not. In the latter case, causality implies  $\mathbf{E} = 0, \mathbf{B} = 0$  when the shortest distance to the emissive part of the cathode is larger than  $ct$ . This necessary property is not at all obvious in field analytical expressions; it will be verified in numerical applications.

The field expressions given below are relative to points located inside the beam, the latter being entirely extracted ( $t > \tau$ ).

### 3.1. The longitudinal electric field $\mathbf{E}_{||} = -\nabla\Phi$

$$E_{z||}(R, Z, T) = -\frac{2I}{\pi\epsilon_0 c A g} \sum_{p=1}^{\infty} \frac{\cos(kpz)}{kp} \cdot \left\{ \int_{\max(0, T-T)}^T \sin[kp(\sqrt{1+u^2}-1)] du \right\} \cdot \begin{cases} 1 - Akp K_1(Akp) I_0(Rkp) & 0 \leq R \leq A \leq \rho \\ Akp I_1(Akp) K_0(Rkp) & 0 \leq A \leq R \leq \rho \end{cases}$$

$$E_{r||}(R, Z, T) = \frac{2I}{\pi\epsilon_0 c A g} \sum_{p=1}^{\infty} \sin(kpz) \cdot \left\{ \int_{\max(0, T-T)}^T \sin[kp(\sqrt{1+u^2}-1)] du \right\} \cdot \begin{cases} K_1(Akp) I_1(Rkp) & 0 \leq R \leq A \leq \rho \\ I_1(Akp) K_1(Rkp) & 0 \leq A \leq R \leq \rho \end{cases}$$

### 4.2. Transverse electric field $\mathbf{E}_{\perp} = -\partial\mathbf{A}/\partial t$ , and magnetic field $\mathbf{B} = B_{\theta} \mathbf{u}_{\theta}$

$$E_{z\perp}(R, Z, T) = -\frac{I}{\pi\epsilon_0 c A g} \int_0^{\infty} J_0(Rx) J_1(Ax) \cdot \left\{ \int_0^T \cos[x(T-T')] \cdot \left[ \sqrt{1+T'^2} - \sqrt{1+(T'-T)^2} \right] dT' + 2 \sum_{p=1}^{\infty} \frac{x^2 \cos(kpz)}{kp(x^2+k^2p^2)} \cdot \int_0^T \cos[\sqrt{x^2+k^2p^2}(T-T')] \cdot \left[ \sin[kp(\sqrt{1+T'^2}-1)] - \sin[kp(\sqrt{1+(T'-T)^2}-1)] \right] dT' \right\} dx.$$

$$E_{r\perp}(R, Z, T) = -\frac{2I}{\pi\epsilon_0 c A g} \int_0^{\infty} x J_0(Rx) \cdot \sum_{p=1}^{\infty} \frac{\sin(kpz)}{k^2 p^2} \cdot m_{Akp} \left( \frac{x}{kp} \right) \left\{ \int_0^T \cos[\sqrt{x^2+k^2p^2}(T-T')] \cdot \left[ \sin[kp(\sqrt{1+T'^2}-1)] - \sin[kp(\sqrt{1+(T'-T)^2}-1)] \right] dT' \right\} dx.$$

where :

$$m_{\alpha}(v) = K_1(\alpha) \int_0^{\alpha} u J_0(uv) I_1(u) du + I_1(\alpha) \int_{\alpha}^{\infty} u J_0(uv) K_1(u) du$$

$$B_{\theta}(R, Z, T) = -\frac{2\mu_0 I}{\pi A g} \int_0^{\infty} x \left\{ J_1(Ax) J_1(Rx) \int_0^T \sin[x(T-T')] \cdot \left[ \sqrt{1+T'^2} - \sqrt{1+(T'-T)^2} \right] dT' + \sum_{p=1}^{\infty} \frac{\cos(kpz)}{kp \sqrt{x^2+k^2p^2}} \cdot \left[ J_0(Rx) m_{Akp} \left( \frac{x}{kp} \right) + 2 \frac{x^2}{x^2+k^2p^2} J_1(Ax) J_1(Rx) \right] \cdot \left[ \sin[kp(\sqrt{1+T'^2}-1)] - \sin[kp(\sqrt{1+(T'-T)^2}-1)] \right] dT' \right\} dx.$$

## 4. APPLICATION TO THE "ELSA" PHOTOINJECTOR : SAMPLE FIELD MAPS

The photoinjector of the "ELSA" facility (CEA, PTN, Bruyères-le-Châtel) has a wide range of possible working parameters. As an example, the chosen parameter set, used for some wake field maps presented below, is :

$$E_0 = 30 \text{ MV/m}, I = 100 \text{ A}, \pi a^2 = 1 \text{ cm}^2, \tau = 30 \text{ ps}$$

Fig. 1 a and b show the total axial E-field  $E_z$ , for  $t = \tau$  : a) on the beam axis, as a function of  $z$ , and b) on the cathode, as a function of  $r$ .

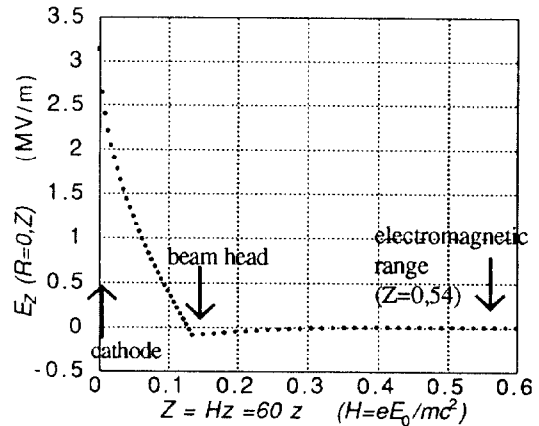


Fig. 1 a.  $E_z$  wakefield on the beam axis, as a function of  $z$ , for  $t = \tau$

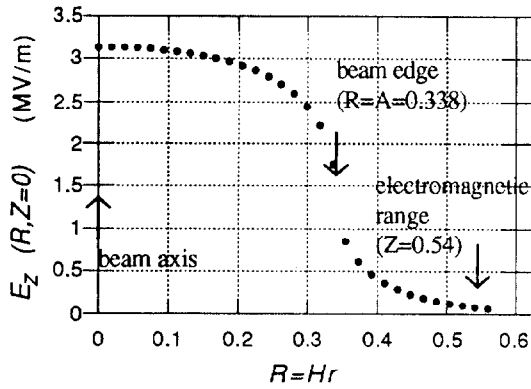


Fig. 1 b.  $E_z$  wakefield on the cathode, as a function of  $r$ , for  $t=\tau$

Fig. 2 shows  $E_z(R=0, Z)$  for  $t=t_g/2$ , where  $t_g$  is the time at which the beam front reaches the anode.

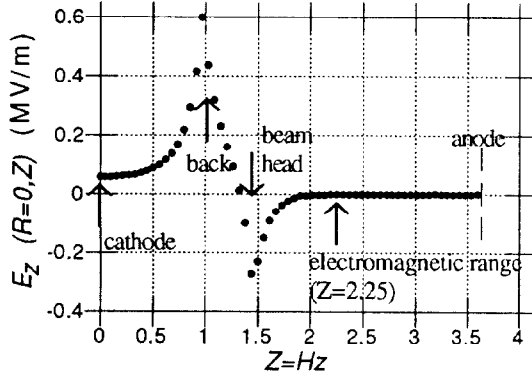


Fig. 2.  $E_z$  wakefield on the beam axis, as a function of  $z$ , for  $t=t_g/2$

Fig. 3 shows, for  $t=t_g/2$ , the radial electric wakefield  $E_r$ , for various  $R=Hr$ , as a function of  $Z=Hz$

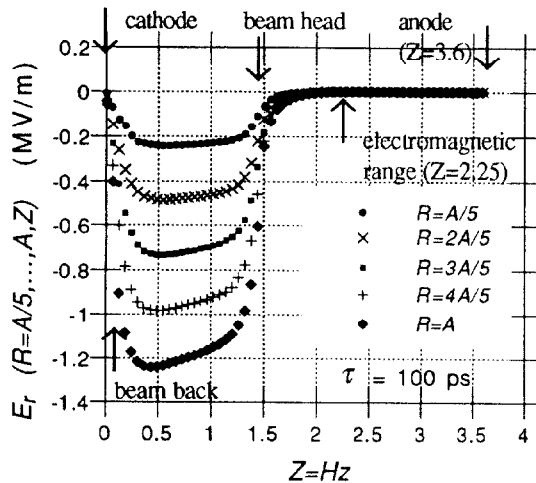


Fig. 3.  $E_r$  wakefield for various  $R=Hr$ , as a function of  $z$  for  $t=t_g/2$

Fig. 4 shows the  $B_\theta$  wakefield for  $r=a/5$ , as a function of  $Z=Hz$

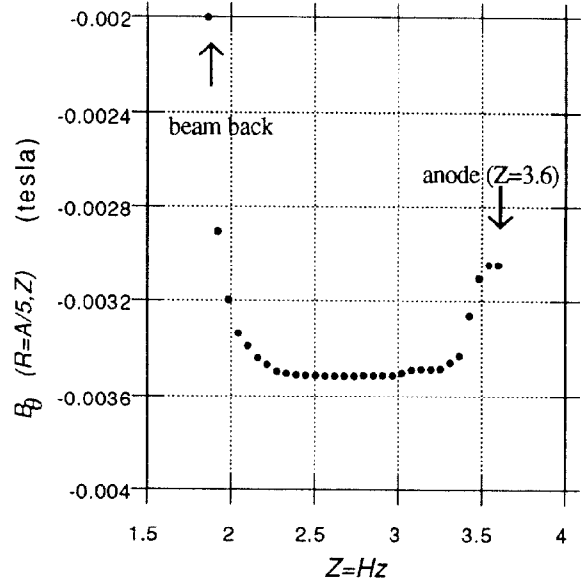


Fig. 4.  $B_\theta$  wakefield for  $r=a/5$ , as a function of  $Z=Hz$

## 5 REFERENCES

- [1] J.-M. Dolique and W. Salah, EPAC 94.
- [2] R. DeiCas, S. Joly *et al.*, Nucl. Instr. Meth. A **318**, 121 (1992).
- [3] T. Weiland, Nucl. Instr. Meth. **212**, 13 (1983).